Vol. 16, No. 2 (2017) 617-624

Materiales

Revista Mexicana de Ingeniería Química

CONCENTRATION EFFECT OF CHROMIUM NANOFLUIDS IN THEIR THERMAL AND OPTICAL PROPERTIES

EFECTOS DE CONCENTRACIÓN DE NANOFLUIDOS DE CROMO SOBRE SUS PROPIEDADES ÓPTICAS Y TÉRMICAS

A. Bahrami[1]*, R. Raoufi[2], K. Behzad[3]

[1] *Department of Physics, Islamshahr Branch, Islamic Azad University, Islamshahr, Iran.*

[2] *Department of Physics, Ahwaz Branch, Islamic Azad University, Ahwaz, Iran.*

[3] *Department of Physics, Shahr-e-Qods Branch, Islamic Azad University, Tehran, Iran.*

Received January 20, 2016; Accepted April 5, 2017

Abstract

In the present investigation chromium nanoparticles at different mass fractions were dispersed in ethylene glycol to have chromium nanofluids. The UV-Vis spectroscopy and transmission electron microscopy results verified that the nanoparticles (NPs) uniformly distributed in the base liquid. Thermal and optical properties of the prepared nanofluids were investigated using photoacoustic spectroscopy and minimum deviation methods. Ethylene glycol, ethanol, and distilled water were used as standard liquids to optimise the experimental setup. The effective thermal effusivity and the refractive index of chromium nanofluids, in ethylene glycol, were measured and the effects of mass fractions were clarified. The results showed that NPs significantly enhance the thermal and optical properties of the investigated nanofluids.

Keywords: thermal effusivity, refractive index, chromium, nanofluid, photoacoustic spectroscopy, minimum deviation.

Resumen

En la presente investigación, se dispersan nanopartículas de cromo en etilen-glicol a diferentes fracciones másicas para tener nanofluidos de cromo. Los resultados de la espectroscopía UV-Vis y microscopía electronica de transmisión verificaron que las nanopartículas (NPs) se distrobuyeron uniformement en el liquid base. Las propiedades térmicas y ópticas de los nanofluidos preparados se investigaron usando espectroscopía fotoacústica y métodos de desviación mínima. Se usaron etilen-gliocl, etanol y agua destilada como líquidos estándar para optimizar el diseño experimental. La efusividad térmica efectiva y el índice de refracción de los nanofluidos de cromo, en etilen-glicol, fueron medidos y los efectos de las fracciones másicas fueron clarificados. Los resultados motraron que las NPs aumentan significativamente las propiedades térmicas y ópticas de los nanofluidos investigados.

Palabras clave: efusividad térmica, índice de refracción, cromo, nanofluido, espectrocopía fotoacústica, desviación mínima.

1 Introduction

According to the definition of nanotechnology, nanoparticles (NPs) size should be less than 100 nm (Pitaksuteepong, 2015). The discovery of novel materials, phenomena, and processes at the nano-scales are the evolution of theoretical and experimental techniques for the evolution of nanosystems and nanostructures materials (Malmonge *et al*., 2010). The use of nanotechnology to develop heat-transfer materials is a rapidly growing topic of research around the world. Nanofluids are one of the mentioned materials that shown promise in the laboratory to dramatically improve thermal conductivity (Faraji *et al*., 2013, Maranville *et al*., 2006). Suspension of appropriate nanoparticles in a conventional heat transfer fluids results in notable enhanced thermal properties (Jiang *et al*., 2015, Jiménez-Pérez *et al*., 2015). These properties of thermal conductivity, thermal diffusivity, viscosity, and design parameter for convective heat transfer are enhanced in comparison to base fluid properties (Esfe *et al*., 2015, Mariano *et al*., 2015), and these results would be beneficial in saving equipment costs and increasing performance (Lazarus

* *Corresponding author. E-mail*: afarin.bah@gmail.com
Tel. 00-98-21-56358105

et al., 2015). Based on the photoacoustic theory, the light energy can be converted to the acoustic wave that is known as the photoacoustic effect. This method was developed by Rosencwaig and Gersho to measure the thermal parameters in liquids and solids (Poulet *et al*., 1980, Sundar *et al*., 2013). Nanofluid can be prepared by dispersing an appropriate amount of NPs in a base fluid (Mortazavi *et al*., 2013). So there are three most important factors in any nanofluids; type of NP, base fluid, and NP concentration. Based on the literature reviews, different properties of the nanofluids were changed by varying the base fluid (Hossain *et al*., 2015, Philip *et al*., 2012). Metal-based NPs such as chromium, cadmium, silver and so on, due to surface plasmon resonance, have strong absorption in the visible range (Basheer *et al*., 2015, Hossain *et al*., 2015). This property got much attention from the researchers due to the unique properties such as high thermal conductivity (Sadrolhosseini *et al*., 2013), thermal collector (Leong *et al*., 2016), and antibacterial activity (Hansen *et al*., 1972, Mollick *et al*., 2014). Thermal effusivity is a measure of nanofluid's ability to exchange heat with its surroundings. Thermal effusivity of various metal-based nanofluids was reported in recent years (Benamrani *et al*., 2011, Hossain *et al*., 2015, Kharazmi *et al*., 2015). The majority of nanofluid thermal conductivity information stated in liquid literature reveals that increasing the NP mass fraction causes an increase in nanofluid's conductivity which announces a linear relationship between the mass fraction of NPs and nanofluid's thermal conductivity (Kang *et al*., 2006, Li *et al*., 2006). The thermal conductivity and thermal effusivity relation is given as (J.Philip, 2003, Stratakis, 2009).

$$\varepsilon = \sqrt{k\rho C} \tag{1}$$

where ε is the thermal effusivity, k is the thermal conductivity, ρ and C are respectively density and the specific heat capacity. Since conductivity, density and thermal effusivity are in direct relationships as shown by Eq.1, it is expected that thermal effusivity increases by an increase in the mass fraction concentration of NPs.

Refractive index is another essential quantity which has various applications in different fields, for instance, it is used in photonic. Since the thermal effusivity and refractive index need to be measured for particular applications of nanofluids (Eastman, 2001).

Water, oil and ethylene glycol were used as heat transfer liquids, so in this work ethylene glycol was chosen as base fluid for Cr nanofluids. The thermal and optical characterizations were carried out to verify the dependency of thermal effusivity and refractive index on mass fraction concentration of Cr nanofluid, using photoacoustic spectroscopy and minimum deviation method.

2 Theory

Rosencwaig - Gersho theory known as R-G theory adequately explains the photoacoustic signal generation in a cell resulting from the absorbed light energy (Rosencwaig, 1976). By passing the chopped laser beam through the cell's window, solid sample was illuminated and the heat intensity is generated at depth x of sample. A sample holder was placed on the photoacoustic (PA) cell and modulated laser beam is focused on the underside of the sample holder, made of Al foil that plays as an interface layer between liquid sample and air in the PA cell. Using Rosencwaig and Gersho model δp that is the air pressure can be calculated as it was expressed well in papers published previously by Delgado-Vaesallo and Marin (Delgado-Vasallo *et al*., 1999) and Delgado-Vaesallo *et al*. (Delgado-Vasallo *et al*., 2000).

$$\delta p = \frac{\beta I_0 \gamma P_0}{2\sqrt{2} k_S l \alpha T_0 (\beta^2 - \sigma_{Al}^2)} F \tag{2}$$

where γ is the specific heat ratio, ε, α and k are respectively thermal effusivity, thermal diffusivity and conductivity of Al. I_o and T_0 are the intensity and temperature, P_0 and β are ambient pressure and optical absorption coefficient of the solid respectively and σ_{Al} is the complex thermal diffusion coefficient. F is the pressure fluctuation made by the Al foil, then:

$$F = \frac{2r}{\sigma_{Al} l_{Al} \left(1 + \frac{2B}{\sigma_{Al} l_{Al}}\right)} \tag{3}$$

where $r = (1 + i)\beta/(2a)$ and a is the parameter which defines as $a = l_s \sqrt{\pi/\alpha_s}$ (O Delgado-Vasallo *et al*., 1999). The reference signal can be measured when the sample holder is empty and given as:

$$|\delta P_{Al}| = \frac{P_1}{f^{P_2}} \tag{4}$$

where p_1 and p_2 are constants, and f is chopping frequency, while in the presence of a sample the amplitude of Eq.2, can be expressed as

$$|\delta P| = \frac{P_1}{f^{P_2} \left(1 + \frac{P_3}{\sqrt{f}} + \frac{P_3^2}{2f}\right)^{1/2}} \tag{5}$$

where P_3 is also constant. Finally, solution thermal effusivity (ε_s) can be simply calculated by fitting based on the below equation.

$$\varepsilon_s = \frac{P_3 \varepsilon_{Al} l_{Al}}{2} \left(\frac{\pi}{\alpha_{Al}} \right)^{1/2} \tag{6}$$

3 Materials and methods

3.1 Preparation of samples

For preparing the Cr nanofluid, Cr NPs with average diameter of 40 nm, from Nano Structured and Amorphous Materials Inc. (USA), and the Ethylene Glycol from Aldrich (Germany) as base fluid were used. To have a uniform nanofluid, the NPs were suspended in ethylene glycol by sonication technique. The appropriate amounts of Cr NP were used to prepare six nanofluids with different mass fraction concentrations of 0.036, 0.072, 0.090, 0.181, 0.272, and 0.381 % (w/w). The solution were mixed in an ultrasonic bath for about 5 hours using Acetyl Trimethyl Ammonium Bromide (CTAB) as surfactant to produce uniform and homogeneous nanofluids.

3.2 Experimental setup

Photoacoustic setup: All the PAS setups consist of three parts: light source, detector, and data analysing system. A Melles Griot HeNe laser of 632.8 nm at power of 75mW was used as a light source that was modulated by Stanford Research Systems optical chopper SR540; a handmade open photoacoustic cell (OPC) was used as a detector. A Stanford Research Systems low-noise preamplifier, SR560, amplified the very weak output signal from OPC and sent it to a Stanford Research Systems lock-in amplifier SR530. The lock-in amplifier and the chopper were controlled using a Lab VIEW program via a GPIB bus as shown in Fig.1 (Faraji *et al*., 2013).

The photoacoustic cell was constructed using Aluminium rod and a Quartz plate was applied as the optical window. When the laser illuminated the nanofluid placed on sample holder with chopped laser beam, the heat transferred to Al foil and heats the air in the cell alternatively. The alternation of heat generates the pressure wave, and the sound was detected using a sensitive microphone. Pre and lock-in amplifiers amplified the pressure variations which were displayed and recorded using a personal computer.

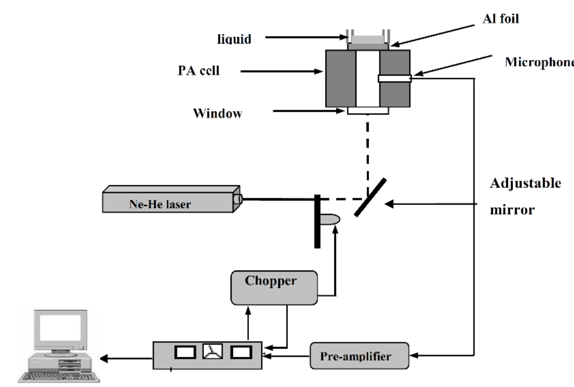

Fig. 1. The experimental set up of open photoacoustic spectroscopy for liquid samples.

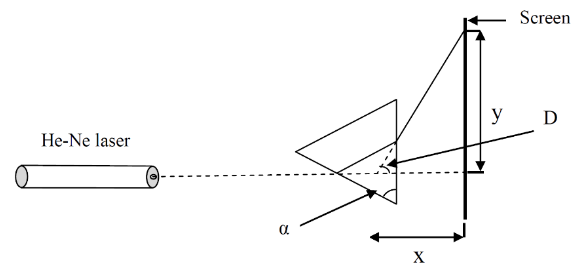

Fig. 2. The experimental set up for measuring refractive index of liquids.

Minimum deviation method: for measuring refractive index the minimum deviation method was used by application of a He-Ne laser (Melles Griot, 632.8 nm), rotation stage, and a hollow prism. By measuring the x and y distances, refractive index (n) can be calculated using the following equation:

$$n = \frac{\sin \frac{1}{2}(\alpha + D)}{\sin(\alpha/2)} \tag{7}$$

where D is deviation angle and α which is the angle of the hollow prism was equal to 60º in present study. The experimental set up of minimum deviation method is presented in Fig. 2. All the measurements were carried out at room temperature about 25ºC.

4 Results and discussion

Fig. 3 shows the optical absorption of six Cr nanofluids that were characterized using UV-Vis spectroscopy. This result reveals that the absorption peaks appeared at 304 nm as it was expected for Cr NPs (Alrehaily, 2015), and the intensity of absorption peaks increases by increasing the concentration of Cr NP in the base fluid (0.036 % to 0.381 %).

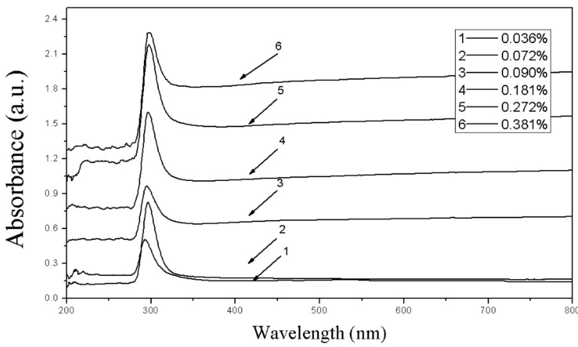

Fig. 3. UV-Vis spectra of Cr nanofluids in different mass fraction concentrations.

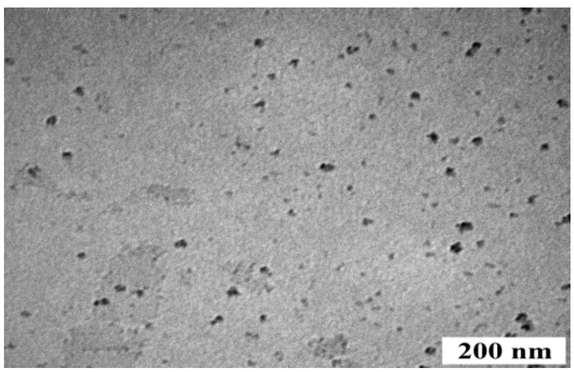

Fig. 4. TEM image of 0.090 % (w/w) Cr NP suspended in ethylene glycol.

The homogeneous distribution of Cr NPs in ethylene glycol after 6 hours sonication in presence of CTAB was verified using transmission electron microscopy (TEM). Fig. 4 is a typical TEM image of the 0.090% nanofluid. TEM images reveal that the Cr NPs dispersed homogeneously in the base fluid.

The measurement of refractive index using minimum deviation method was verified by measuring the refractive indexes of standard liquids. The refractive index of distilled water, ethanol, and ethylene glycol were measured and the values are respectively equal to 1.327, 1.359 and 1.427 which agreed well with the reported values (Aralaguppi *et al*., 1999, Deirmendjian, 1964, Dostalek *et al*., 2005, Sasaki *et al*., 1991). In photoacoustic setup the sample holder made by Al foil. Regarding to Eq.6 first of all, it needs to measure the thermal diffusivity of Al using photoacoustic spectroscopy. The obtained value was 0.939 cm^2/s, this value is in good agreement with the literature values (Behzad, Mat Yunus, Talib, Zakaria and Bahrami, 2012, Behzad, Mat Yunus, Talib, Zakaria, Bahrami, *et al*., 2012). Using the measured thermal effusivity of empty sample holder, the constant parameters (p_1, p_2) were calculated. Before measuring the thermal effusivity of nanofluids and for calibrating the photoacoustic spectroscopy set up, the thermal effusivity values of Di water, ethanol, and ethylene glycol, as standard samples, were measured and the obtained values are 0.163, 0.054 and 0.093 $Ws^{1/2}/cm^2K$ respectively. The measured values for standard samples also are in good agreement with the reported values (Balderas-Lopez, 2007, Sylvain Delenclos, 2002). After ensuring the accuracy of the data, Cr nanofluids were thermally characterized using the photoacoustic spectroscopy. Generally, the thermal effusivity and refractive index of nanofluids are higher than those of the base fluids (Ali *et al*., 2010). Fig. 5a and Fig. 5b show the PA intensity signal as function of frequency for two nanofluids with the Cr mass fractions of 0.036 and 0.090% (w/w), respectively. The solid curve represents the best fit of the theoretical data.

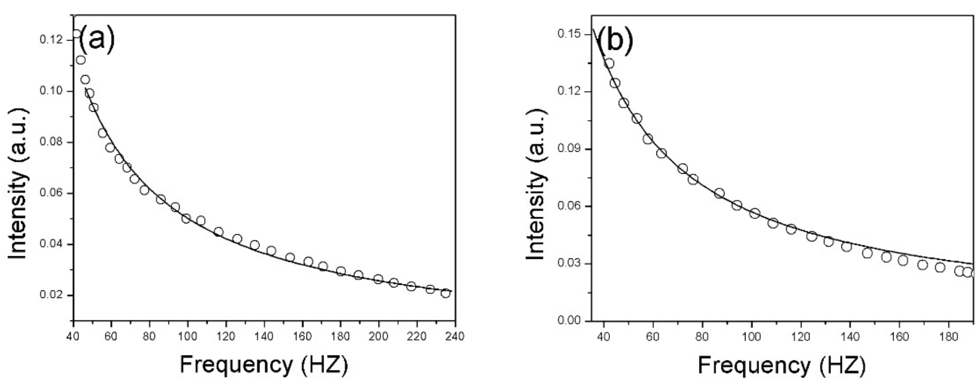

Fig. 5. Intensity dependent on the frequency variations obtained by photoacoustic spectroscopy for (a) 0.036 % and (b) 0.090 % (w/w) Cr NPs suspended in EG.

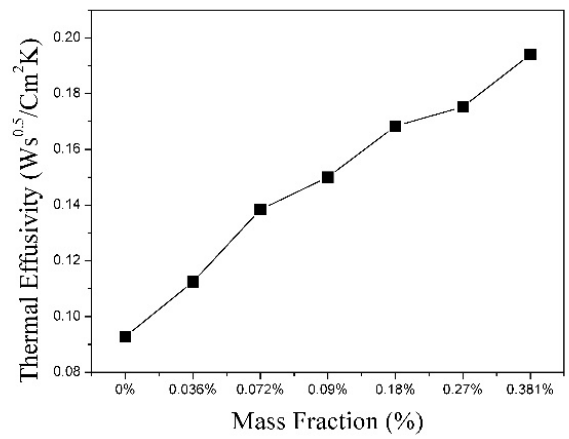

Fig. 6. Variation of thermal effusivity versus mass concentration of Cr NPs.

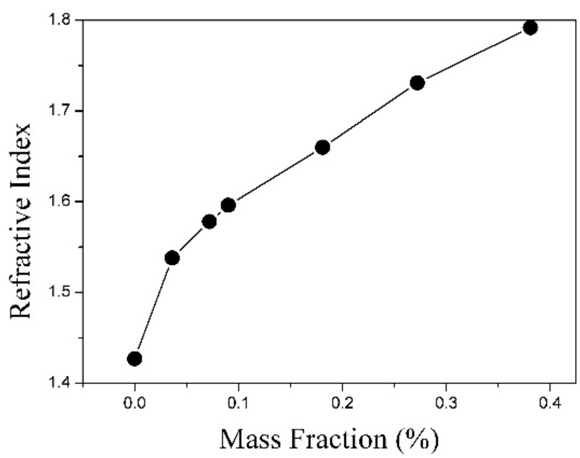

Fig. 7. Variation of refractive index versus mass concentration of Cr NPs.

Fig. 6 shows the variation of thermal effusivity as function of mass fraction of Cr nanofluids. This figure reveals that thermal effusivity of ethylene glycol (0%) slightly increase from 0.093 to 0.112 ($Ws^{1/2}/cm^2$ K) by adding of 0.036% Cr NPs. Thermal effusivity increases almost linearly by adding more NPs up to 0.194 ($Ws^{1/2}/cm^2$ K) for the nanofluid of 0.381% NPs.

The figure shows a considerable increase in thermal effusivity by increasing the mass fraction. The results show a 109% increase in thermal effusivity of ethylene glycol by turn it into Cr nanofluid of 0.381%.

Fig. 7 reveals the refractive index of Cr nanofluid as function of mass fraction concentration. Refractive index shows a considerable change by converting the ethylene glycol to Cr nanofluid. Refractive index almost linearly, increases from 1.538 to 1.792 by increasing the mass fraction from 0.036 to 0.381%.

Table. 1. Thermal effusivity and refractive index of Cr nanofluids.

Mass fraction of Cr NP (%)	**Thermal effusivity ($Ws^{1/2}/cm^2$ K)**	**Refractive index**
0.000	0.093	1.427
0.036	0.112	1.538
0.072	0.138	1.578
0.090	0.150	1.596
0.181	0.168	1.660
0.272	0.175	1.731
0.381	0.194	1.792

Thermal effusivity and refractive index show higher values in Cr nanofluids in compare with the base fluid due to increase of NPs in nanofluids. Table 1 shows the thermal effusivity and refractive index values for all nanofluids.

Conclusions

Six Cr nanofluids with different mass fraction concentrations of 0.036, 0.072, 0.090, 0.181, 0.272, and 0.381% (w/w) were prepared by dispersing the Cr NPs in ethylene glycol. Thermal effusivity and refractive index of Cr nanofluids were successfully measured using photoacoustic spectroscopy and minimum deviation methods respectively. Thermal effusivity of nanofluids increased from 0.112 to 0.194 $Ws^{1/2}/cm^2$ K and the refractive index values roughly linearly increased from 1.538 to 1.792 by increasing the mass fraction concentration. This research revealed that tuning the thermal effusivity and refractive index of Cr nanofluids are possible by varying the mass fraction concentration of NPs to use as a coolant or liquid optical devices.

Acknowledgements

We acknowledge the Islamshahr Branch of Islamic Azad University for providing the research facilities for us to carry out this research.

References

Ali, F. M., Yunus, W. M. M., Moksin, M. M., and Talib, Z. A. (2010). The effect of volume fraction concentration on the thermal conductivity and thermal diffusivity of nanofluids: numerical and experimental. *Review of Scientific Instruments 81*, 074901.

Alrehaily, L. M. 2015. Gamma-Radiation Induced Redox Reactions and Colloidal Formation of Chromium and Cobalt Oxide Nanoparticles, The University of Western Ontario.

Aralaguppi, M. I., Jadar, C. V., and Aminabhavi, T. M. (1999). Density, Viscosity, Refractive Index, and Speed of Sound in Binary Mixtures of Acrylonitrile with Methanol, Ethanol, Propan-1-ol, Butan-1-ol, Pentan-1-ol, Hexan-1-ol, Heptan-1-ol, and Butan-2-ol. *Journal of Chemical & Engineering Data 44*, 216-221.

Balderas-Lopez, J. A. (2007). Thermal effusivity measurements for liquids: A self-consistent photoacoustic methodology. *Review of Scientific Instruments 78*, 064901.

Basheer, N. S., Kumar, B. R., Kurian, A., and George, S. D. 2015. Thermal conductivity measurement of organic solvents incorporated with silver nanoparticle using photothermal techniques. Paper read at IOP Conference Series: Materials Science and Engineering.

Behzad, K., Mat Yunus, W. M., Talib, Z. A., Zakaria, A., and Bahrami, A. (2012). Preparation and Thermal Characterization of Annealed Gold Coated Porous Silicon. *Materials 5*, 157-168.

Behzad, K., Mat Yunus, W. M., Talib, Z. A., Zakaria, A., Bahrami, A., and Shahriari, E. (2012). Effect of Etching Time on Optical and Thermal Properties of p-Type Porous Silicon Prepared by Electrical Anodisation Method. *Advances in Optical Technologies* 2012.

Benamrani, H., Satour, F. Z., Zegadi, A., and Zouaoui, A. (2011). Photoacoustic spectroscopy analysis of silicon crystals. Journal of Luminescence. *Journal of Luminescence 132*, 305-312.

Deirmendjian, D. (1964). Scattering and polarization properties of water clouds and hazes in the visible and infrared. *Applied Optics 3*, 187-196.

Delgado-Vasallo, O., and Marin, E. (1999). The application of the photoacoustic technique to the measurement of the thermal effusivity of liquids. *Journal of Physics D: Applied Physics 32*, 593.

Delgado-Vasallo, O., and Marín, E. (1999). The application of the photoacoustic technique to the measurement of the thermal effusivity of liquids. *Journal of Physics D: Applied Physics 32*, 593.

Delgado-Vasallo, O., Valdés, A. C., Marín, E., Lima, J. A. P., Da Silva, M. V. S., Sthel, M., Vargas, H., and Cardoso, S. L. (2000). Optical and thermal properties of liquids measured by means of an open photoacoustic cell. *Measurement Science and Technology 11*, 412.

Dostalek, J., Homola, J., and Miler, M. (2005). Rich information format surface plasmon resonance biosensor based on array of diffraction gratings. *Sensors and Actuators B: Chemical 107*, 154-161.

Eastman, J. A. (2001). Anomalously increased effective thermal conductivities of ethylene gelycol-based nanofluids containing copper nanoparticles. *IEEE Xplore 76*, 718-720.

Esfe, M. H., Karimipour, A., Yan, W.-M., Akbari, M., Safaei, M. R., and Dahari, M. (2015). Experimental study on thermal conductivity of ethylene glycol based nanofluids containing Al_2O_3 nanoparticles. *International Journal of Heat and Mass Transfer 88*, 728-734.

Faraji, N., Yunus, W. M. M., Kharazmi, A., Saion, E., and Behzad, K. (2013). Open Photoacoustic Cell Configuration Applied to the Thermal Characterization of Liquid CdS Nanocomposites. *International Journal of Thermophysics*, 1-9.

Hansen, D., and Bernier, G. A. (1972). Thermal conductivity of polyethylene: The effects of crystal size, density and orientation on the thermal conductivity. *Polymer Engineering & Science 12*, 204-208.

Hossain, M. S., Saidur, R., Sabri, M. F. M., Said, Z., and Hassani, S. (2015). Spotlight on available optical properties and models of nanofluids: A review. *Renewable and Sustainable Energy Reviews 43*, 750-762.

J.Philip, R. R. a. (2003). Memory switching in In-Te glasses: results of heat-transport measurements. *Semiconductor Science and Technology 18*, 133-138.

Jiang, H., Xu, Q., Huang, C., and Shi, L. (2015). Effect of temperature on the effective thermal conductivity of n-tetradecane-based nanofluids containing copper nanoparticles. *Particuology 22*, 95-99.

Jiménez-Pérez, J. L., López-Gamboa, G., Cruz-Orea, A., and Correa-Pacheco, Z. N. (2015). Thermal parameters study of biodiesel containing Au nanoparticles using photothermal techniques. *Revista Mexicana de Ingeniería Química 14*, 481-487.

Kang, H. U., Kim, S. H., and Oh, J. M. (2006). Estimation of thermal conductivity of nanofluid using experimental effective particle volume. *Experimental Heat Transfer 19*, 181-191.

Kharazmi, A., Faraji, N., Hussin, R. M., Saion, E., Yunus, W. M. M., and Behzad, K. (2015). Structural, optical, opto-thermal and thermal properties of ZnS-PVA nanofluids synthesized through a radiolytic approach. *Beilstein Journal of Nanotechnology 6*, 529-536.

Lazarus, G., Roy, S., Kunhappan, D., Cephas, E., and Wongwises, S. (2015). Heat transfer performance of silver/water nanofluid in a solar flat-plate collector. *Journal of Thermal Engineering 1*, 104-112.

Leong, K., Ong, H. C., Amer, N., Norazrina, M., Risby, M., and Ahmad, K. K. (2016). An overview on current application of nanofluids in solar thermal collector and its challenges. *Renewable and Sustainable Energy Reviews 53*, 1092-1105.

Li, C. H., and Peterson, G. P. (2006). Experimental investigation of temperature and volume fraction variations on the effective thermal conductivity of nanoparticle suspensions (nanofluids). *Journal of Applied Physics 99*, 084314.

Malmonge, L. F., Langiano, S. d. C., Cordeiro, J. M. M., Mattoso, L. H. C., and Malmonge, J. A. (2010). Thermal and mechanical properties of PVDF/PANI blends. *Materials Research 13, 465-470.*

Maranville, C., Ohtani, H., Sawall, D., Remillard, J., and Ginder, J. 2006. Thermal Conductivity Measurements in Nanofluids via the Transient Planar Source Method. SAE Technical Paper.

Mariano, A., Pastoriza-Gallego, M. J., Lugo, L., Mussari, L., and Piñeiro, M. M. (2015). Co 3 O 4 ethylene glycol-based nanofluids: thermal conductivity, viscosity and high pressure density. *International Journal of Heat and Mass Transfer 85*, 54-60.

Mollick, M. M. R., Bhowmick, B., Maity, D., Mondal, D., Roy, I., Sarkar, J., Rana, D., Acharya, K., Chattopadhyay, S., and Chattopadhyay, D. (2014). Green synthesis of silver nanoparticles-based nanofluids and investigation of their antimicrobial activities. *Microfluidics and nanofluidics 16*, 541-551.

Mortazavi, B., Bardon, J., and Ahzi, S. (2013). Interphase effect on the elastic and thermal conductivity response of polymer nanocomposite materials: 3D finite element study. *Computational Materials Science 69*, 100-106.

Philip, J., and Shima, P. D. (2012). Thermal properties of nanofluids. *Advances in Colloid and Interface Science 183-184*, 30-45.

Pitaksuteepong, T. (2015). Nanotechnology: effective topical delivery systems. *Asian Journal of Pharmaceutical Sciences*.

Poulet, P., Chambron, J., and Unterreiner, R. (1980). Quantitative photoacoustic spectroscopy applied to thermally thick samples. *Journal of Applied Physics 51*, 1738-1742.

Rosencwaig, A. (1976). Theory of the photoacoustic effect with solids. Journal of Applied Physics. *Journal of Applied Physics 47*, 64-69.

Sadrolhosseini, A. R., Noor, A., Shameli, K., Kharazmi, A., Huang, N., and Mahdi, M. (2013). Preparation of graphene oxide stabilized nickel nanoparticles with thermal effusivity properties by laser ablation method. *Journal of Nanomaterials 2013*, 144.

Sasaki, K., Koshioka, M., Misawa, H., Kitamura, N., and Masuhara, H. (1991). Pattern formation and flow control of fine particles by laser-scanning micromanipulation. *Optics Letters 16*, 1463-1465.

Stratakis, E., Barberoglou, Marios, Fotakis, Costas, Viau, Guillaume, Garcia, Cecile, Shafeev, Georgy A. (2009). Generation of Al nanoparticles via ablation of bulk Al in liquids with short laser pulses. *Optics Express 17*, 12650-12659.

Sundar, L. S., Farooky, M. H., Sarada, S. N., and Singh, M. K. (2013). Experimental thermal conductivity of ethylene glycol and water mixture based low volume concentration of Al_2O_3 and CuO nanofluids. *International Communications in Heat and Mass Transfer 41*, 41-46.

Sylvain Delenclos, M. C., Abdelhak Hadj Sahraoui, Corinne Kolinsky, Jean Marc Buisine. (2002). Assessment of calibration procedures for accurate determination of thermal parameters of liquids and their temperature dependence using the photopyroelectric method. *Review of Scientific Instruments 73*, 2773-2780.